Interfacial Rheology of Surface-Active Biopolymers: *Acacia senegal* Gum versus Hydrophobically Modifed Starch

Philipp Erni,*,† Erich J. Windhab,† Rok Gunde,† Muriel Graber,† Bruno Pfister,† Alan Parker,‡ and Peter Fischer†

Institute of Food Science and Nutrition and Materials Research Center, ETH Zürich, CH-8092 Zürich, Switzerland, and Firmenich SA, 7 Rue de la Bergère, CH-1217 Meyrin 2, Geneva, Switzerland

Received May 24, 2007; Revised Manuscript Received August 30, 2007

Acacia gum is a hybrid polyelectrolyte containing both protein and polysaccharide subunits. We study the interfacial rheology of its adsorption layers at the oil/water interface and compare it with adsorbed layers of hydrophobically modified starch, which for economic and political reasons is often used as a substitute for Acacia gum in technological applications. Both the shear and the dilatational rheological responses of the interfaces are considered. In dilatational experiments, the viscoelastic response of the starch derivative is just slightly weaker than that for Acacia gum, whereas we found pronounced differences in shear flow: The interfaces covered with the plant gum flow like a rigid, solidlike material with large storage moduli and a linear viscoelastic regime limited to small shear deformations, above which we observe apparent yielding behavior. In contrast, the films formed by hydrophobically modified starch are predominantly viscous, and the shear moduli are only weakly dependent on the deformation. Concerning their most important technological use as emulsion stabilizers, the dynamic interfacial responses imply not only distinct interfacial dynamics but also different stabilizing mechanisms for these two biopolymers.

Introduction

Acacia gum, or "gum arabic", is a hybrid polyelectrolyte containing both protein and polysaccharide components. It is a natural plant exudation collected from *Acacia* trees and one of the most prevalent industrial gums.[1] Currently, it is used, mostly on an empirical basis, in the food industry, in particular for beverage and flavor oil emulsions, in pharmaceutical emulsions, as well as in adhesive, paper, textile, and other industries. Its popularity is primarily due to its capacity as an interfacial stabilizer ("emulsifier") upon adsorption at liquid interfaces, combined with good solubility in aqueous systems, enabling the use of gum arabic as a viscosity enhancer.[2] Acacia gum has also been shown to be a very efficient stabilizing agent for single-walled carbon nanotubes.[3] In this latter application, the gum physically adsorbs at the liquid/solid surface and facilitates redispersing of dried nanotube suspensions; this principle has been applied for thousands of years in the preparation of carbon black ink.[4] The origin of industrial gum arabic stretches over a wide semiarid belt ("gum belt") in sub-Saharan Africa with Sudan being the largest producer, followed by Nigeria, Chad, Mali, and Senegal.[1] Among more than 1000 known species of *Acacia*, which are further divided into several varieties, the most abundant species is *Acacia senegal*, which is also systematically cultivated. Lesser amounts of some commercial gums originate from *Acacia seyal*, and trade products often contain gum collected from several botanical species. Several detailed overviews of plant exudate gums, their biochemistry, physicochemical properties, as well as historic, economic, and legislative aspects exist.[1,4−8]

The polysaccharide backbone of Acacia gum is composed of 1,3-linked β-galactopyranose monomers and 1,6-linked galactopyranose side chains, terminated either by glucuronic acid or by 4-*O*-methylglucuronic acid residues. The minor protein component is covalently linked to the polysaccharide via its serine and hydroxyproline side chains, forming arabinogalactan−protein/peptide complexes with multiple polysaccharide blocks sharing a protein core. It is now recognized that gum arabic mainly consists of three fractions:[1,6,7,9−12] (i) The most abundant portion by weight (around 88.4% w/w of the total gum) is an arabinogalactan (AG) fraction[11,12] with a mean molecular weight around $M_W \approx 2.79 \times 10^5$ g mol^{-1}. (ii) A high-molecular-weight ($M_W \approx 1.45 \times 10^6$ g mol^{-1}) arabinogalactan−protein (AGP) complex fraction, with its suggested "wattle blossom" type structure, is considered the most surface-active fraction and is expected to play an important role for the emulsion-stabilizing properties of Acacia gum. (iii) A third minor glycoprotein fraction contributes around 1.2% w/w of the gum. Recently, some of the most detailed data so far on the physical and chemical features of *Acacia senegal* gum have been provided by Renard et al.;[12] on the basis of data obtained with a variety of techniques, including hydrophobic interaction chromatography, multiangle laser light scattering, biochemical analyses, and others, these authors conclude that the plant gum is indeed a continuum of molecular species with varying sugar ratios, molecular weights, and charges. Al-Assaf et al.[9] performed a detailed study on the molecular weight of dozens of samples of *Acacia senegal* gum and found extensive variation between individual samples. Idris et al.[10] used multidetection gel permeation chromatography to characterize the gums from *Acacia* trees of various origins and ages; whereas they found the highest molecular weights for the oldest trees, no significant regional differences were observed in that study. Furthermore, these authors noted that for the integral gum the monosaccharide

* Author to whom correspondence should be addressed. Current address: Hatsopoulos Microfluids Laboratory, Massachusetts Institute of Technology, Cambridge, MA 02139. E-mail: erni@mit.edu

† ETH Zürich.

‡ Firmenich SA.

10.1021/bm700578z CCC: $37.00
Published on Web 10/20/2007

composition, protein and amino acid content, as well as the optical rotation did not show any obvious trends with either origin or age of the trees. From the perspective of plant molecular biology, considerable progress has been made in structural analysis of arabinogalactan−proteins and the understanding of their functionality.[13]

Dickinson et al.[14] measured steady interfacial shear viscosities of gum arabic at the oil/water interface; they presented a method to exchange the subphase liquid during measurements and found that if the aqueous subphase is diluted, then changes in surface viscosity are only small and occur on very long time scales up to 100 h. This supports the notion that at least a fraction of gum arabic is very resilient to desorption from the liquid interface, similar to the desorption behavior of some surface-active proteins. Another important result by these authors suggests a strong correlation between the amount of proteinaceous components within gum arabic and the interfacial rheology of its adsorption layers. Randall et al.[11] fractionated gum arabic by size exclusion chromatography and showed that indeed the proteinaceous component provides most of the surface activity of Acacia gum. Ducel et al.[15] studied the interfacial properties of plant protein/Acacia gum coacervataes at the oil/water interface; they focused on interfacial compression/dilatation experiments performed with the pendant drop method. A number of studies have been concerned with combined systems involving both proteins and plant gums; most of these focus on bulk solution properties[16] as well as phase separation and coacervation;[17−19] some studies also address the interfacial activity of combined plant gum/protein systems.[15,20] A shear rheological study of interfaces covered with Acacia exudate gums was performed by Elmanan et al.;[21] these authors studied the time-dependent interfacial storage and loss moduli in oscillatory interfacial shear flow. Earlier results[22] also indicated that the interfacial elasticity increased as a function of both concentration and time. These studies did not go into further detail with respect to the deformation and frequency dependence of the interfacial moduli. Lopez-Franco et al.[23] compared two different plant gums, those from *Acacia* spp. and mesquite gum from *Prosopis velutina* in terms of their surface pressure−area isotherms measured in the Langmuir film balance. Sanchez et al.[24] peformed rheological measurements on Acacia gum dispersions; they argued that the observed apparent non-Newtonian behavior and viscoelasticity may to some extent be due to interfacial rheological effects present at the free surface of the samples. While these authors did not perform surface shear rheology, they did study the response of the interfaces to dilatation/compression deformations in a pendant drop tensiometer. Fauconnier et al.[25] studied surface layers of gums from *Acacia senegal* and *Acacia seyal* in the Langmuir film balance and found that the former forms more elastic films than the latter if a static elasticity derived from the surface pressure−area isotherm is considered. Surface chemical aspects of Acacia gums have also been discussed in the broader context of hydrocolloid emulsifiers[5−7,16] for pharmaceutical and food systems.

Whereas Acacia gum offers ideal properties both as a thickening agent and as a surface-active biopolymer, problems arise with raw material variability across regions as well as trade and political issues, both of which complicate quality control in technological applications. However, only a few native polysaccharides exhibit interfacial activities comparable to Acacia gum. Therefore, if alternative materials are to be used, then amphiphilic properties must be introduced specifically by targeted modification of the biopolymer, for example, by grafting appropriate side groups on a cellulose[26] or starch[8] backbone. Recently, covalent conjugates of whey proteins with maltodextrin have been suggested as an alternative to gum arabic.[27] Among alternatives to replace Acacia gums, hydrophobically modified starch has been the most successful in applications where stabilization of liquid interfaces is desired, in particular for use in emulsions in the beverage and flavor industry.[8] A common modification of the starch source involves substitution with nonpolar alkenyl succinate side groups to impart partial hydrophobicity and, therefore, surface activity onto the amylopectin fraction of the starch. Starch modification with octenyl succinic anhydride ("OSA−starch-") was patented in 1953.[28,29] Nowadays, starch octenyl succinate derivatives are commercially available and used in numerous applications involving oil/water interfaces. Areas of application include the pharmaceutical,[30] food,[8,31−34] and other[36,35] industries. Bao et al.[29] investigated octenyl succinic anhydride starches derived from different sources, including rice, wheat, and potato starches, and showed that besides the degree of side chain substitution the physical properties, such as viscosities, gel strengths, or swelling volumes, strongly depend on the botanical origin of the starches. Bhosale and Singhal[37] studied the emulsification capacity of OSA−starches derived from waxy maize and amaranth. Jansson and Järnström[35] investigated the barrier and mechanical properties of modified starches in the context of paper and textile coatings. Nilsson and Bergenståhl[33] studied the adsorption of hydrophobically modified starch at oil/water interfaces during emulsification; they estimated interfacial concentrations of OSA starch using the serum depletion method and found surface loads up to 16 mg m^{-2}. These authors also present a model that treats the macromolecular adsorption process as a collision between particles in turbulent flow with the consequence that the adsorption time of a polymer decreases with increasing polymer radius. The correlation of the degree of substitution in octenyl succinate starch with its capacity as an emulsion stabilizer was studied by Viswanathan.[34] Hydrophobically modified starches in the context of flavor emulsions for the food industry were reviewed by Trubiano.[8] Chanamai and McClements[31] compared the capacities of gum arabic and hydrophobically modified starch to flocculate emulsions by depletion; they found that the critical flocculation concentration of gum arabic is lower due to its higher effective volume.

Among the physicochemical properties of both Acacia gum and hydrophobically modified starch, three main aspects are of particular interest for technological applications: (i) They act as viscosity enhancers; however, compared to other common biopolymers used as stabilizers, the thickening capacity is rather limited, and both biopolymers are not commonly used as gel formers. (ii) Both biopolymers are surface-active; they adsorb to to oil/water interfaces and decrease the interfacial tension. (iii) Interfacial adsorption layers formed by Acacia gum exhibit considerable stresses if the interface is deformed laterally, both under shear and compression/dilatation deformations. In the present article, we focus on the third aspect, which, given its potential significance and with the exceptions cited above, has still received comparably minor attention.

Interfacial rheology ("two-dimensional (2D) rheology") is the study of the deformation and flow of adsorption layers at oil/water or air/water interfaces.[38−40] Whereas it is sufficient to characterize clean, surfactant-free liquid interfaces with a static interfacial tension, the description of interfaces containing surface-active species must take into account the mass and momentum transport processes occurring during formation, deformation, or breakup of liquid interfaces. In analogy to bulk rheology, the total surface stress at a liquid interface is composed

of an isotropic portion, the "surface pressure" $\Pi = \sigma_0 - \sigma$, and an extra stress, $\bar{\tau}$, the latter of which is a tensorial quantity. σ is the interfacial tension with the index 0 denoting the reference tension of the clean interface. Consequently, the interfacial extra stress has the units of force length^{-1}, just as the interfacial tension. Notice the analogy to the stress and hydrostatic pressure in three-dimensional systems with units of force length^{-2}. Interfacial rheology is usually subdivided into the fields of shear rheology and dilatational rheology. The former involves shearing deformations of an interfacial area element while retaining its area; the latter describes the changes of the interfacial stress upon changes in size of an interfacial area element while retaining its shape by either compressing or dilating it. In many applications, such as emulsion and foam stability, drop or bubble deformation in multiphase flow, etc., both deformation modes exist.[38] Several material functions are used to characterize liquid interfacial layers: the steady interfacial shear viscosity η and dilatational viscosity κ (both in units of N m^{-1} s), measured in steady interfacial shear flow or compression/dilatational flow. If oscillatory flows are used to study the interfaces, then the viscosities are replaced by the complex dilatational and shear viscosities of the interface, containing both the viscous and the elastic components. Alternatively, in the modulus notation, the interfacial shear moduli G' (elastic) and G'' (viscous) and dilatational moduli E' (elastic) and E'' (viscous) are used, as a function both of the strain γ and of the angular frequency of the oscillations ω. We will discuss the following surface rheological parameters: the transient relaxation modulus $G(t) = \tau_s/\gamma_0$, the interfacial shear moduli G' (elastic) and G'' (viscous), and the magnitude of the corresponding complex shear viscosity $|\eta^*|$.

Our overview suggests that by now much progress has been made in advancing the structural knowledge of Acacia gum and its individual fractions, including their surface activities. In terms of the interfacial functionality of plant gums, previous studies have focused on the steady shear viscosity as well as the dilatational rheological behavior of Acacia gum, both as integral gum as well as for individual fractions. However, despite recent advances in more detailed molecular characterization of plant exudate gums, a comprehensive interfacial rheological study of gum arabic, involving the frequeny dependence of the interfacial elastic and viscous moduli, the behavior at small and large strains, the time-dependent evolution of interfacial viscoelasticity, as well as comparison with transient rheological experiments (creep and stress relaxation), is still missing. Furthermore, no direct comparison has yet been made between the interfacial rheology of Acacia gum and the behavior of its most common replacement in technological applications, hydrophobically modified starch. In this article, we describe the dynamic interfacial rheology of Acacia gum in both shear and dilatational deformations, and we compare it to results obtained with octenyl succinate anhydride starch (hydrophobically modified starch from waxy maize). We first summarize the instrumentation and methods, including interfacial shear rheometry (using the biconical disk method) as well as interfacial compression/dilatational rheology (using the oscillating pendant drop method). Experimental results for Acacia gum are presented for various rheological test functions in shear mode: dynamic shear at variable frequencies and deformation amplitudes, transient shear under creep and stress relaxation conditions, as well as the time-dependent evolution of the moduli. Measurements of the interfacial dilatational modulus and the transient interfacial tension are presented. Throughout the article, we will compare the rheological responses of Acacia gum and hydrophobically modified starch.

Materials and Methods

Materials. Gum arabic (IRX 49.345, *Acacia senegal* gum, purified, Colloïdes Naturels International, Rouen, France) was kindly provided by Albert Isliker & Co. (Zurich, Switzerland). Hydrophobically modified starch (derived from waxy maize starch, Purity Gum BE, National Starch, Bridgewater, NJ) was provided by Select-Chemie (Zurich, Switzerland). For an in-depth characterization of Acacia gums, we refer to a recent article in this journal.[12] All of the biopolymer dispersions were produced with purified water (Milli-Q) and filtered (0.45 μm pore size, Nalgene Labware). (+)-Carvene (limonene) and chloroform (analysis grade) were obtained from Sigma and used as received. The biopolymer dispersions are hydrated for 12 h under gentle stirring. The densities and dynamic viscosities of the aqueous gum arabic dispersions, all measured at 20 °C, are 1.077 g cm^{-3} and 48 mPa s (at a biopolymer concentration $c = 20\%$ w/w) and 1.037 g cm^{-3} and 11 mPa s ($c_w = 10\%$ w/w); for hydrophobically modified starch, the values are 1.036 g cm^{-3} and 64 mPa s. The density of the (+)-carvene oil phase is 0.842 g cm^{-3}, and its dynamic viscosity is 0.9 mPa s. The bulk rheological properties of all liquids were measured in a Physica MCR 300 rheometer (Anton Paar, Ostfildern, Germany). For the gum arabic and hydrophobically modified starch dispersions a Couette geometry was used (type CC 27, cylinder diameter 26.66 mm, cup diameter 28.92 mm), while for (+)-carvene a double-wall geometry (type DG 26.7) was chosen, providing better sensitivity at low stresses.

Interfacial Rheology. The interfacial shear moduli G' and G'' are measured in a Physica MCR 300 rheometer equipped with an interfacial rheology measuring cell, based on the biconical disk geometry[39] (Figure 1). A disk is positioned in the region of the phase boundary and is rotated or oscillated, either under a controlled torque, while measuring the resulting deformation, or under an applied deformation or deformation rate, while measuring the resulting torque. For a detailed description we refer to our earlier article focusing on instrumentation aspects.[39] The moduli are calculated using the analysis described in refs 39 and 41. The method is based on the solution of the Stokes equation for the interfacial velocity in the rheometer cup for a rotating biconical disk placed at the interface between two immiscible liquids. A jump mass balance and a jump momentum balance at the interface are used, where the latter contains the Boussinesq−Scriven law for the stress boundary condition at the interface.[42,43] Oh and Slattery[41] have first provided an exact solution for the velocity distribution in steady shear flow in the plane of the interface. The interfacial shear stress, τ, and interfacial shear viscosity, η, are calculated using an iterative procedure from the angular velocity and the disk torque. Dynamic experiments are performed to obtain information on the viscoelastic properties of the interfaces at different rheological time scales.[44] In this case the shear strain γ is varied sinusoidally with time at an angular frequency ω: $\gamma(t) = \gamma_0 \sin(\omega t)$, where t is time and γ_0 is the oscillation amplitude. For linear viscoelastic materials, the response function is a sinusoidally changing shear stress, $\tau(t) = -\tau_0 \sin(\omega t + \phi)$, that is out of phase with the strain. A complex shear modulus $G^* = G' + iG''$ can be defined from the stress and strain waves as $G^* = \tau_0 e^{i\phi}/\gamma_0$ with ϕ being the phase angle. The storage modulus, G', then describes the elastic properties of the sample, while the loss modulus, G'', is proportional to the viscous resistance. Alternatively, viscoelasticity can be probed using transient experiments. In stress relaxation experiments, the time-dependent rheological response of the shear stress $\tau(t)$ to a given step strain function of the deformation is measured. In creep experiments, a constant stress is imposed onto the sample during a defined time, and the deformation response function during this stress pulse (creep curve) is measured. Additionally, this experiment provides information about the recovery behavior of the strain upon removal of the stress. The material function defined from creep experiments is called the creep compliance $J(t) = \gamma(t)/\tau_0$ and is defined as the ratio of the time-

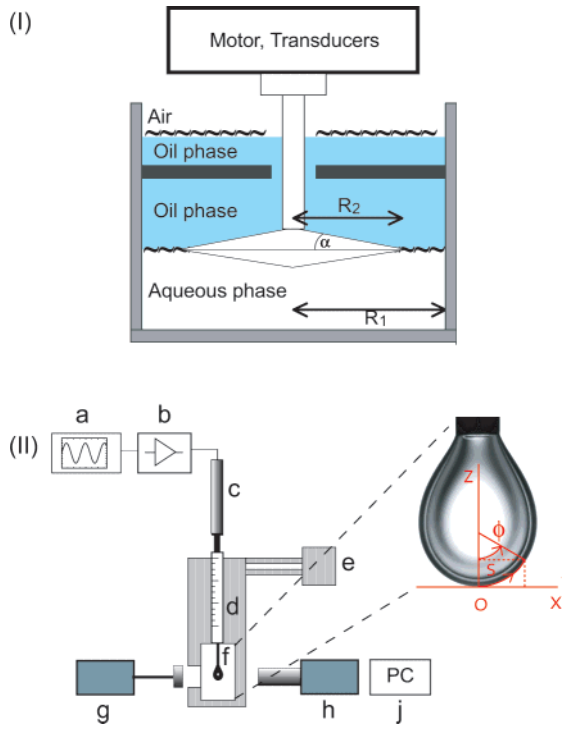

Figure 1. Schematic of the interfacial rheometrical methods used in this work (not to scale). (I) Interfacial shear rheometer with a rotating biconical disk shown at an oil/water interface (R_1, disk diameter, 34.14 mm; R_2, cup diameter, 40 mm; α, cone angle, 5°). (II) Oscillating pendant drop tensiometer (a, function generator; b, amplifier; c, piezoelectric actuator; d, glass syringe; e, heating/cooling system for cuvette and syringe; f, sample cell containing the continuous phase; g, light source with glass fiber and diffusor; h, CCD camera with macro zoom lens; j, personal computer for image acquisition and data analysis). The inset shows the parametrization of the drop contour used to calculate interfacial tensions in the pendant drop tensiometer.

dependent deformation and the imposed stress pulse. For all experiments performed with the interfacial rheometer, the measuring cell is cleaned consecutively with hot water, ethanol, and chloroform before and after every measurement. The surface of the lower liquid is sucked clean with an aspirator immediately before the disk is brought into contact with the liquid; after the disk has been positioned at the surface of the lower liquid (here, the aqueous biopolymer phase), the upper liquid is gently layered on top with a syringe pump-. Note that the torques and deflection angles to be detected in interfacial shear rheometery are of extremely small magnitudes as compared to bulk rheometry; therefore, particular attention must be paid to careful alignment and calibration of the rheometer. Prior to every measurement, the rheometer is aligned horizontally on an optical bench. Once the biconical disk is mounted, the motor is adjusted to compensate for imperfect positioning of the measuring geometry. Such imperfections are inevitable to some extent and can add considerable experimental noise to the low-torque data.

For tensiometry and dilatational rheometry at the oil/water interface, an oscillating pendant drop tensiometer built in our laboratory was used (Figure 1).[45] The principle of the method is to use a pendant or rising drop suspended from a capillary into the continuous liquid phase to obtain a profile image of the drop contour and then fit the theoretical Laplace equation to this experimental profile by a numerical procedure.[45] In addition to equilibrium and dynamic interfacial tension measurements, the device can be used for interfacial dilatational rheometry if the volume of the drop and, therefore, its surface area can be varied in defined ways. A glass syringe is used to generate a pendant drop, and a piezoelectric actuator imposes small changes of volume onto the drop, either in oscillatory or in transient mode. A piezoelectric actuator (PI Instrumente P-840.613) is mounted above the syringe piston and driven by a function generator (Yokogawa

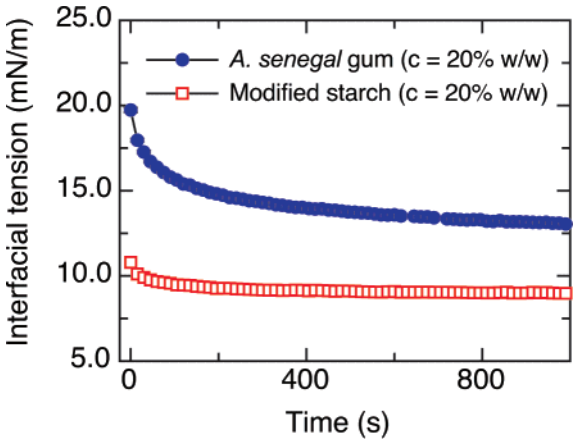

Figure 2. Time-dependent interfacial tension at the interfaces Acacia gum arabic/(+)-carvene and hydrophobically modified starch/(+)-carvene as measured with the pendant drop method (biopolymer concentrations c = 20% w/w, T = 20 °C).

FG 300) via an amplifier (PI Instrumente). A spring-loaded mechanism is used to counterbalance the force exerted by the actuator on the syringe piston. Thermostated water is circulated through a steel housing for the quartz glass cuvette and through a plexiglass block holding the syringe. Two spindle drives are used for rough adjustment to move the syringe plunger and create drops of a desired volume. The dilatational modulus of an interface can be obtained from the surface pressure (Π) and area (A) data as $E = \partial\Pi/(\partial A/A_0)$. A static modulus can be obtained from the slope of the surface pressure−area isotherm. For harmonic area changes, $A(t) = A_0 \exp(-i\omega t)$, where ω is the deformation frequency in rad s^{-1}, the dilatational modulus is a complex quantity, $E^*(w) = E' + iE''$, with a real part E' (storage or elastic modulus) and an imaginary part E'' (loss or viscous modulus). If E^* is measured in an experiment involving small sinusdoidal area perturbations, then the moduli are measured in analogy to bulk rheology from the stress response $\Pi(t)$ to a given strain function $\Delta A(t)/A_0$.

Results

In the following, we will discuss the interfacial properties of Acacia gum and hydrophobically modified starch under the most important rheological test functions: dynamic shear flow at variable frequency and deformation amplitude, transient shear flow under creep and stress relaxation conditions, as well as the time-dependent evolution of the viscoelastic moduli. We also address aspects of the dilatational rheology and the transient interfacial tension of the adsorption layers. Figure 2 compares the transient interfacial tensions measured with pendant drops for Acacia gum and modified starch. At identical weight concentrations (which is the relevant parameter for technical applications of both biopolymers) Acacia gum decreases the tension of the oil/water interface to a value around 12.2 mN/m, compared with a value of 8.9 mN/m for modified starch. Both Acacia gum and modified starch are highly nonideal in terms of their solution and adsorption properties: Their molecular weights are high compared to the solvent molecules, molecular conformation upon adsorption cannot be assumed constant, and adsorption has been shown to be effectively irreversible in the case of Acacia gum. Therefore, common surfactant adsorption models are not amenable for the calculation of, for example, the self-diffusion coefficient. Many macromolecular adsorption layers are known to exhibit rheological aging behavior, reflected in a strong time dependence of their viscoelastic moduli. Such behavior has been observed mostly for polypeptides and

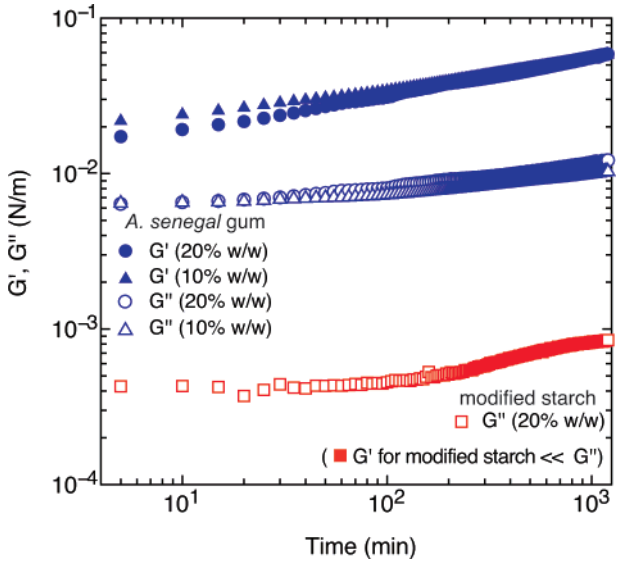

Figure 3. Time dependence of the interfacial shear moduli G' (storage) and G'' (loss) of *Acacia senegal* gum and hydrophobically modified starch at the oil/water interface ($T = 20$ °C, deformation amplitude $\gamma_0 = 1\%$). The storage modulus G' for modified starch was below the detection limit.

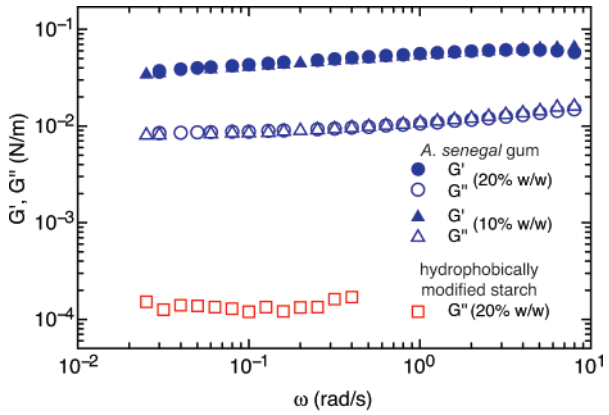

Figure 4. Interfacial shear rheology, frequency dependence of the interfacial shear moduli for Acacia gum and hydrophobically modified starch: G', storage modulus; G'', loss modulus. For the starch layers, G' is below the detection limit at all frequencies (interface age 20 h, strain amplitude $\gamma_0 = 1\%$).

proteins,[7,39,40,46] but it is also relevant for other macromolecules, including plant gums.[21] Aging is influenced by the adsorption/diffusion time scales of macromolecules, especially in the early stages of adsorption; because the gum described here is a mixture of compounds exhibiting complex interactions and is used at relatively high concentrations corresponding to the situation found in real applications, we assume that diffusion-controlled adsorption of a primary interfacial layer is not responsible for the slow growth of the viscoelastic moduli seen here. In contrast, the slow dynamics that are often observed, for example, in globular protein layers, seem to be an intrinsic property for some adsorption layers and can in some cases be interpreted in terms of analogy with bulk "soft glassy" materials, where aging is known as a common feature.[47]

Time-sweep experiments involving oscillatory shear flow are shown in Figure 3. The deformation amplitude and oscillation frequency are held constant at $\gamma_0 = 1\%$ and $\omega = 1$ rad s^{-1}. Data acquisition is started 5 min after the oil phase has been layered on top of the aqueous phase. At this deformation and frequency, Acacia gum layers are elastic ($G' > G''$) even at the earliest data point recorded, whereas the starch derivative remains viscous at all times. The moduli for the two different concentrations are in close agreement; in particular, the storage modulus, which is indicative of the development of a densely packed interfacial layer, is practically independent of the concentration at time scales longer than 2 h. This is likely a result of the large excess of surface-active biopolymer at either concentration. Consequently, we attribute the slightly faster initial growth of the storage modulus of the gum at the lower concentration ($c_w = 10\%$ w/w) to a bulk viscosity effect: Lower bulk viscosity allows faster structure formation in the interface. The aging behavior of hydrophobically modified starch is less characteristic with a moderate increase in the viscous modulus after about 3 h; the increase might be associated with some degree of physical gelation, similar to effects measured with another mostly viscous surface-active biopolymer, β-casein;[48] however, even at the longest time scales, no significant elasticity is measured.

Notice that with the exception of the initial growth in G' for Acacia gum the most pronounced changes in the interfacial shear moduli occur on time scales at which the time-dependent interfacial tension of the layers (Figure 2) has already attained a stationary value or decreases only very weakly—in other words, oscillatory interfacial shear flow is a probe that reveals much more detailed information about the layers than either the static or the transient interfacial tension. We have also monitored the rheology of the subphase on the same time scales relevant to surface aging using bulk rheometry in a concentric cylinder geometry and have not found any relevant changes in the bulk viscoelastic moduli: The subphase rheology remains viscous even at old surface ages. In these control experiments, care was taken to exclude surface rheological contributions to the bulk moduli, which might influence the measurements at the free surface of the liquid. Such artifacts may be observed if a cone/plate fixture is used, where the surface-to-volume ratio of the sample is rather large.

Figure 4 compares the interfacial shear moduli for the two biopolymers after 20 h of aging in the rheometer cell. The moduli were measured over a range of angular frequencies from $\omega(10^{-2})$ to $\omega(10^{1})$ rad s^{-1} at a strain amplitude of 1%. For Acacia gum, the interfacial viscoelastic contribution to the total system response is so strong that the quality of data is excellent over this entire range of time scales. (In interfacial rheology, oscillatory measurements at low frequencies are often problematic due to low total stress levels and, correspondingly, poor signal-to-noise ratios.) Due to the much smaller magnitudes of the shear moduli of the layers formed by hydrophobically modified starch, the accessible frequency range is more narrow for that system, limited by increasingly noisy data at low frequencies and by inertia effects at higher frequencies. The frequency response of the two types of layers is very different and highly characteristic for the individual biopolymer: Acacia gum is elastic ($G' > G''$) at all frequencies measured with a ratio G''/G' corresponding to a loss tangent on the order of tan $\delta \approx 0.2$ and phase angles δ around 10°. Furthermore, both the individual moduli and the loss tangent are essentially scale-free and show very weak dependence on the oscillation frequency. Such behavior has also been observed for globular surface-active proteins[39,40] as well as for interfacial layers of colloidal particles. For those systems, analogy with either "soft glassy" materials or with particulate gel networks has been suggested (depending on the strength of the interaction potential between the particles and the packing fraction).[47,49,50] We also find that if a correct subphase drag correction is applied to the data, then the interfacial shear moduli are independent of the

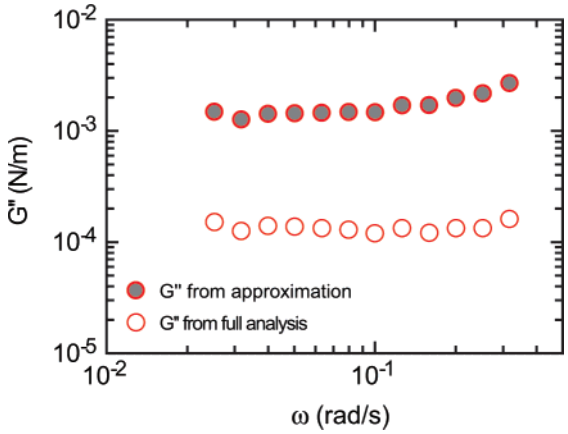

Figure 5. Role of the subphase drag contribution to the interfacial rheology of adsorption layers formed by hydrophobically modified starch. Filled symbols: loss modulus G'' calculated by subtracting a blank value for the subphase stress from the total stress response (interface + bulk), assuming simple additivity of the interface and subphase rheological properties. Open symbols: G'' from full analysis of the interfacial stress,[39,41] accounting for coupled flow between interface and bulk.

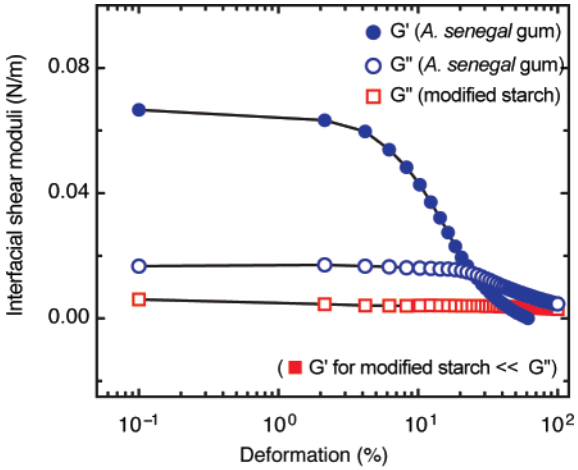

Figure 6. Deformation dependence of the interfacial shear moduli G' and G'' of *Acacia senegal* gum and hydrophobically modified starch at the oil/water interface ($T = 20$ °C, $\omega = 1$ rad s^{-1}, interface age $t_0 = 20$ h).

bulk-phase concentration of the biopolymer; this result further supports our earlier conclusion that the vast excess of surface-active material available in the bulk phase at the two technologically relevant concentrations leaves little significance for the adsorption kinetics that would be relevant at dilute concentrations. The consistent values for the data obtained at the two different bulk-phase concentrations ($c_w = 10\%$ and 20% w/w) further support this conclusion. In contrast, hydrophobically modified starch is purely viscous at the frequencies studied here with viscous moduli G'' on the order of 10^{-4} N/m and elastic moduli G' that are below our detection limit. This system exhibits a very weak shear rheological response, dominated completely by the loss modulus G''. (G' is undetectable in this case, and the phase angle is 90° throughout; therefore the contribution from G'' dominates the total complex modulus $|G^*|$.) For reference, we note that purely viscous interfacial shear responses have been found, for example, for β-casein,[48] a flexible random coil protein, or for fatty alcohol Langmuir monolayers, such as those formed by eicosanol.[51] At low values of the interfacial moduli, it is important to assess the role of the subphase drag contribution the interfacial moduli, in particular if the viscous shear modulus is dominant. Note that the bulk viscosity is higher than that of water (64 mPa s at 20 °C), while the interfacial stresses are rather low; therefore we would expect that the subphase stress contribution is relevant in this example. Indeed, the role of stress dissipation from the interface into the bulk is an open question in many interfacial rheological studies. This is generally an important problem if the ratio of the interfacial viscosity to the bulk viscosity scaled with a characteristic length scale R is small,[39,41,51] i.e., $\eta/(\eta_{bulk}R) < 1$. This ratio is a dimensionless parameter, often named the Boussinesq number; here, R can be set to the radius of the rheometer geometry. Often, the subphase contribution is accounted for by subtracting a blank stress value, measured or calculated with the surfactant-free interface. Whereas comprehensive analyses accounting for flow coupling have been achieved by several authors for many standard flow geometries,[38] they are rarely used for data evaluation, and many authors prefer to use an approximation method that simply subtracts a blank stress value for the subphase from the measured total stress signal (subphase + interface). Figure 5 compares the interfacial loss modulus calculated from both the approximation and the full analysis used here,[39] where the latter correctly accounts for the subphase drag. We find that the blank-corrected values exceed the ones calculated with the full hydrodynamic method[39,41] by more than an order of magnitude; i.e., the interfacial stresses and moduli are overpredicted. Obviously, hydrodynamic coupling with the subphase liquid must be addressed carefully for weak interfacial layers.

Deformation-dependence of the interfacial moduli is an important feature of many viscoelastic adsorption layers. Figure 6 presents strain amplitude sweep experiments for both Acacia gum and modified starch. We find that Acacia gum layers exhibit a linear viscoelastic regime (LVE) only at the smallest deformations studied up to critical strains of approximately $\gamma = 1-2\%$; above this limit, the elastic modulus strongly decreases with deformation. Analogy with rigidlike protein adsorption layers as well as numerous bulk materials such as pastes or concentrated suspensions suggests that Acacia gum is a fragile interfacial network material and that the decrease in elasticity corresponds to structural breakdown; for protein layers, for example, those formed by ovalbumin, it has been observed that this "yielding" behavior coincides with actual fracture events in the layer.[46] For Acacia gum, we can therefore postulate four different regimes for the deformation-dependent interfacial shear rheology, according to the terminology used by Chang et al.:[52] (i) linear viscoelasticity up to $\gamma \approx 1-2\%$, (ii) nonlinear viscoelastic creep flow, (iii) fracture with eventual crossover of G' and G'', and (iv) apparent shear thinning of the ruptured layer at high deformations. Note that with the exception of the linear viscoelastic data measured at small deformations in all of these regimes the shear moduli are apparent quantities, based on the macroscopically measurable rheological quantities. Modified starch, in contrast, does not exhibit any significant strain dependence for the viscous shear modulus. This further supports the view of adsorbed modified starch as a viscous interfacial layer with very minor solid characteristics. To further compare the two materials, we plot the deformation-dependent moduli in a stress−strain diagram based on the values of the oscillatory stress and strain amplitudes from the dynamic experiments, τ and γ. Again, Acacia gum shows the typical response of "soft solid" materials, including a peak stress that can be interpreted as a yield value and subsequent leveling off of the interfacial stress at higher deformations. The inset of Figure 7 also shows that both materials are indeed linear

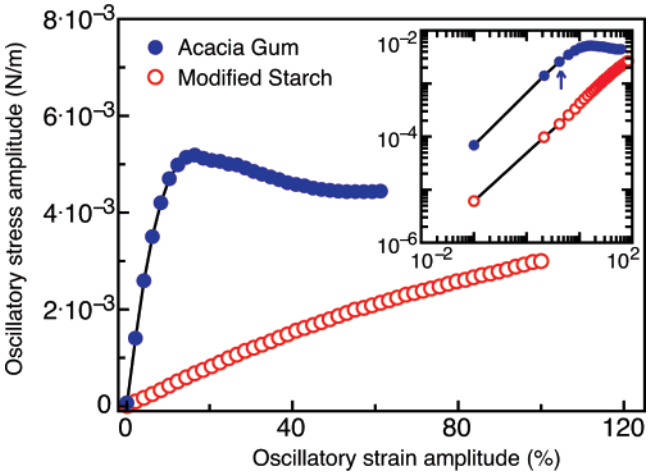

Figure 7. Stress−strain curves for Acacia gum and modified starch, based on oscillatory strain amplitude sweep data (interface age 20 h, oscillation frequency $\omega = 1$ rad s^{-1}). The inset shows the same experiments in a double logarithmic plot to emphasize the linear viscoelastic regime at low strains and deviation from linearity for Acacia gum, as indicated by the arrow.

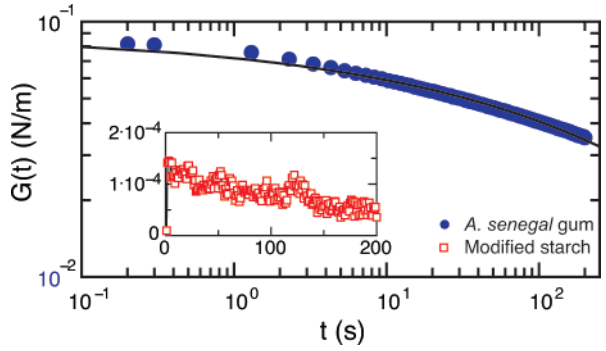

Figure 8. Relaxation of the interfacial shear modulus after a strain step. Interface between Acacia gum vs (+)-carvene, strain step $\gamma_0 =$ 1%. The inset shows the much weaker stress relaxation response of modified starch to the identical strain step ($c_w = 20\%$ w/w in both cases). Line guides the eye.

viscoelastic at low deformations with the deviation from linearity indicated by the arrow.

We proceed to a discussion of interfacial shear viscoelasticity studied in transient deformations (as opposed to oscillatory, frequency-domain experiments). In stress relaxation (or step strain) experiments, the time-dependent response of the stress $\tau(t)$ to a given step function of the deformation γ_- ($t < 0$) to γ_+ ($t \geq 0$) is recorded. Therefore, deformation-controlled rheometers are used for this test to provide sufficiently fast and well-controlled deformation changes. Figure 8 shows the interfacial shear relaxation modulus $G(t \geq 0)$ to a step function of the strain to $\gamma_+ = 1\%$ at time $t = 0$ for both Acacia gum and modified starch. Again, the two surfaces have very different shear responses in this deformation mode also: The plant gum, with an "instantaneous" relaxation modulus on the order of 0.08 N/m, shows considerable shear elasticity and slow relaxation with a slowest relaxation time far above 10^2 s. A fit to a phenomenological power law relaxation law, $G(t) = St^{-n}$, gives values of $S = 0.09$ for the gel strength parameter[44] and $n = 0.182$ for the gel exponent. The latter value is in a range that is rather typical for particular gels, and similar values are found for many bulk systems.[53] For the experiments shown here, other phenomenological models, such as a stretched exponential law, would also provide a good description of the same data. For a true differentiation between weak particulate gels and colloidal

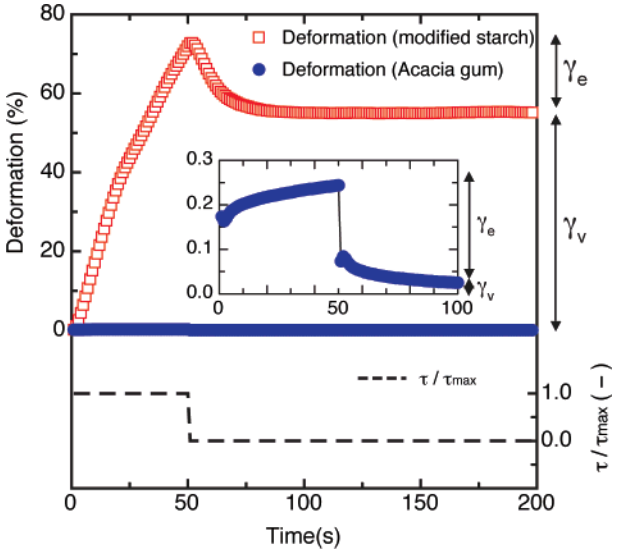

Figure 9. Creep response of Acacia gum and modified starch at the oil/water interface. A torque pulse $M_0 = 0.5$ μN m is imposed onto the interface at time $t = 0$ (dashed line), and the resulting deformation is measured. The main graph compares both biopolymers; the inset magnifies the creep data for Acacia gum to emphasize both the pronounced instantaneous elastic jump in deformation and the much more solidlike creep portion of the data. The arrows on the right-hand side indicate the elastically recovered strain γ_e and the viscous portion γ_v.

glasses,[49,50] additional information about the actual microstructure in the layer, including an interfacial packing fraction, as well as about the strength of the colloidal interactions is necessary. Modified starch shows a stress relaxation response almost 3 orders of magnitude weaker than that of the plant gum (inset of Figure 8); these values for the relaxation modulus are indeed near the detection limit of our measurements, but unlike in the oscillatory experiments it is still possible to detect some minimum degree of elasticity with this kind of measurement. Note that for a clean interface $G(t)$ is zero throughout.

The transient behavior can also be investigated using the creep test, in which a constant stress is imposed onto the sample during a defined time, and the strain response during this stress pulse (creep curve) is recorded. Additionally, this experiment provides information about the recovery behavior of the strain upon removal of the stress. Whereas oscillatory measurements did not allow us to detect the elastic component of the modulus for modified starch (undetectable G' due to the low total torques and values for the phase angles around 90°), the creep recovery curve gives a much clearer picture of the relative importance of the viscous and elastic moduli, and this measurement therefore provides us with quantitative information on the elastic contribution to the modulus in adsorbed layers of hydrophobically modified starch. Figure 9 compares the strain responses of both biopolymers to an imposed torque pulse of 0.5 μN m, held for 50 s. In the main graph both responses are plotted on the same scale. The most striking difference for the two materials is the pronounced difference in the absolute magnitudes of their strain response: Acacia gum is restricted to only minor strains below $\gamma = 0.3\%$, whereas modified starch flows more easily and reaches strains on the order of 75% after 50 s. In both cases, a phase of steady shear flow is reached within 50 s, as indicated by the linear growth of $\gamma(t)$ with time. (In this case, the steady shear viscosity of the interface can be derived from the slope of the creep curve.) We further note a much more pronounced instantaneous jump in deformation for Acacia gum, confirming the solidlike nature of its adsorption layers (inset graph in Figure

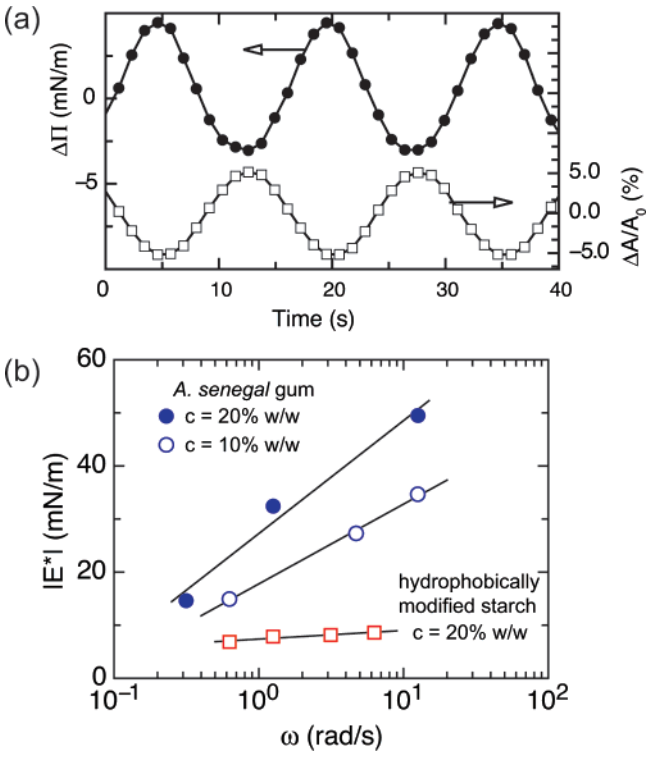

Figure 10. (a) Interfacial dilatational rheology: typical surface pressure response in an oscillatory experiment. $\Delta\Pi(t)$ is the change in surface pressure, and $\Delta A/A_0(t)$ is the incremental area change resulting from a sinusoidally varying drop volume. (b) Dilatational moduli of *Acacia senegal* gum and hydrophobically modified starch adsorbed at the oil/water interface, measured with the oscillating pendant drop method.

9). A third important piece of information can be read from the ratio of the elastically recovered strain γ_e to the dissipative (viscous) strain γ_v: For Acacia gum, γ_e/γ_v is on the order of 17.7, whereas for modified starch it is 0.35, indicating pronounced elasticity for the former and viscous behavior for the latter. Finally, creep experiments also provide us with an easily conceivable picture about the flow behavior of the Acacia gum layers below a critical stress ("yield stress"): The nonzero slope of the creep curve during the stress pulse indicates that the layer indeed flows, in agreement with the non-negligible viscous modulus measure in the oscillatory experiments; therefore it is more appropriate to describe the behavior around the yield point as a flow transition from a predominantly elastic material response with a non-negligible viscous component to an apparently shear-thinning regime at higher stresses and strains.

The dilatational moduli $|E^*|$ of Acacia gum and hydrophobically modified starch were measured under oscillatory area changes $\Delta A/A_0$ at the oil/water interface. An exemplary set of raw data for the temporal surface pressure response $\Delta\Pi(t)$ is shown in Figure 10a. In Figure 10b, the dilatational moduli of the two biopolymers at the oil/water interface are summarized. In all cases a strong dilatational response is observed with the relative magnitude of the modulus following the same order as in the shear experiments: Acacia gum exhibits a higher dilatational moduli than hydrophobically modified starch with values increasing at higher concentrations and exceeding the moduli of modified starch by about an order of magnitude at comparable concentrations.

Although the dilatational modulus of hydrophobically modified starch is smaller than that for Acacia gum, its magnitude is still considerable—indeed, the dilatational rheology of these two systems seems to be rather similar on a qualitative basis. This is in stark contrast to the results measured in shear deformation, where the starch layers exhibit only very weak rheological responses and are predominantly viscous. On the basis of a review of the literature on both shear and dilatational rheology of adsorbed polymer layers, we suggest an analogy with adsorbed, surface-active proteins: Acacia gum is in many ways reminiscent of globular protein layers, such as those formed by β-lactoglobulin or ovalbumin. (We do not infer similarities in molecular structure but rather point out the related interfacial rheological responses.) Hydrophobically modified starch, however, with its similar dilatational response but weak and elasticity-free shear rheology might be grouped along random coil adsorbed polymers, such as β-casein, where physical gelation or 2D glassy behavior is only expected to play a minor role. For the two systems studied here, a correlation with the intrinsic molecular "hardness"[46] will obviously be very difficult due to the presence of various molecular species, but the analogy with globular and flexible surface-active proteins may be helpful for further insight. Interfacial shear rheology is therefore a sensitive method to probe highly structured, rigid layers, while dilatational interfacial rheology, however, provides a measure of the ability of the interface to adapt to a change in concentration (either by adsorption/desorption or by in-plane relaxation).

Summary and Conclusions

An overall comparison of the rheology of the adsorption layers of Acacia gum and hydrophobically modified starch at the oil/water interface reveals highly characteristic mechanical properties of those two materials. Additionally, it also suggests that the efficiency of each of these biopolymers in their most common application, the stabilization of oil/water interfaces in emulsions, may be due to different physicochemical mechanisms: For Acacia gum, the mechanical stability of the adsorption layer is expected to play a significant role, reflected by substantial shear elasticity of the interface. In contrast, the absence of interfacial rigidity suggests that in the case of hydrophobically modified starch the functionality as an emulsion stabilizer is due to other effects which, besides the ability to decrease interfacial tension, would include surface charge, steric stabilization, and surface tension gradient effects. The latter are indeed reflected in the considerable dilatational modulus of modified starch, shown in Figure 10. It should also be noted that the adsorption conditions present in our experiment might be different from the situation found in an emulsification process, where freshly created portions of interface are not quiescent during the initial loading with the macromolecular emulsifiers. According to Nilsson and Bergenståhl,[33] interfacial concentrations of modified starch are typically in the range of 1−3 mg m^{-2} but can be as high as 16 mg m^{-2}, in which case those authors suggest interfacial "jamming". However, in the experiments shown above, the absence of a pronounced interfacial shear elasticity for modified starch indicates that such effects would presumably not be found here. The dynamic interfacial rheological responses imply different stabilizing mechanisms of Acacia gum and modified starch: Acacia gum produces strong, viscoelastic interfacial films, whereas the interfacial functionality of hydrophobically modified starch is more traditional in terms of a macromolecular surfactant.

Acknowledgment. P.E. acknowledges financial support from the Swiss National Science Foundation (SNF Project No. 2100-065976).

CDV

References and Notes

(1) Islam, A. M.; Phillips, G. O.; Sljivo, A.; Snowden, M. J.; Williams, P. A. *Food Hydrocolloids* **1997**, *11*, 493−505.
(2) Tan, C.-T. In *Food Emulsions*, 4th ed.; Friberg, S. E., Larsson, K., Sjöblom, J., Eds.; Marcel Dekker: New York, 2004; pp 485−524.
(3) Bandyopadhyaya, R.; Nativ-Roth, E.; Regev, O.; Yerushalmi-Rozen, R. *Nano Lett.* **2002**, *2*, 25−28.
(4) Verbeken, D.; Dierckx, S.; Dewettinck, K. *Appl. Microbiol. Biotechnol* **2003**, *63*, 10−21.
(5) Garti, N. *J. Dispersion Sci. Technol.* **1999**, *20*, 327−355.
(6) Garti, N.; Leser, M. E. *Polym. Adv. Technol.* **2001**, *12*, 123−135.
(7) Dickinson, E. *Food Hydrocolloids* **2003**, *17*, 25−39.
(8) Trubiano, P. C. In *Flavor Technology: Physical Chemistry, Modification, and Process*; Ho, C.-T., Tan, C.-T., Tong, C.-H., Eds.; ACS Symposium Series 610; American Chemical Society: Washington, DC, 1995; pp 199−209.
(9) Al-Assaf, S.; Phillips, G. O.; Williams, P. A. *Food Hydrocolloids* **2005**, *19*, 647−660.
(10) Idris, O. H. M.; Williams, P. A.; Phillips, G. O. *Food Hydrocolloids* **1998**, *12*, 379−388.
(11) Randall, R. C.; Phillips, G. O.; Williams, P. A. *Food Hydrocolloids* **1988**, *2*, 131−140.
(12) Renard, D.; Lavenant-Gourgeon, L.; Ralet, M. C.; Sanchez, C. *Biomacromolecules* **2006**, *7*, 2637−2649.
(13) Gaspar, Y.; Johnson, K. L.; McKenna, J. A.; Bacic, A.; Schultz, C. J. *Plant Mol. Biol.* **2001**, *47*, 161−176.
(14) Dickinson, E.; Elverson, D. J.; Murray, B. S. *Food Hydrocolloids* **1989**, *3*, 101−114.
(15) Ducel, V.; Richard, J.; Popineau, Y.; Boury, F. *Biomacromolecules* **2005**, *6*, 790−796.
(16) Huang, X.; Kakuda, Y.; Cui, W. *Food Hydrocolloids* **2001**, *15*, 533−542.
(17) Scholten, E.; Sagis, L. M. C.; van der Linden, E. *J. Phys. Chem. B* **2004**, *108*, 12164−12169.
(18) Schmitt, C.; Sanchez, C.; Lamprecht, A.; Renard, D.; Lehr, C. M.; de Kruif, C. G.; Hardy, J. *Colloids Surf., B* **2001**, *20*, 267−280.
(19) Weinbreck, F.; Wientjes, R. H. W.; Nieuwenhuijse, H.; Robijn, G. W.; de Kruif, C. G. *J. Rheol.* **2004**, *48*, 1215−1228.
(20) Ibanoglu, E. *J. Food. Eng.* **2002**, *52*, 273−277.
(21) Elmanan, M.; Al-Assaf, S.; Phillips, G. O.; Williams, P. A. *Food Hydrocolloids*, in press.
(22) Burgess, D. J.; Sahin, N. O. *J. Colloid Interface Sci.* **1997**, *189*, 74−82.
(23) Lopez-Franco, Y. L.; Valdez, M. A.; Hernandez, J.; de la Barca, A. M. C.; Rinaudo, M.; Goycoolea, F. M. *Macromol. Biosci.* **2004**, *4*, 865−874.
(24) Sanchez, C.; Renard, D.; Robert, P.; Schmitt, C.; Lefebvre, J. *Food Hydrocolloids* **2002**, *16*, 257−267.
(25) Fauconnier, M. J.; Blecker, C.; Groyne, J.; Razafindralambo, H.; Vanzeveren, E.; Marlier, M.; Paquot, M. *J. Agric. Food Chem.* **2000**, *48*, 2709−2712.
(26) Fischer, P.; Brooks, C. F.; Fuller, G. G.; Ritcey, A. R.; Xiao, Y., Rahem, T. *Langmuir* **2000**, *16*, 726−734.
(27) Akhtar, M.; Dickinson, E. *Food Hydrocolloids* **2007**, *21*, 607−616.
(28) Caldwell, C. G.; Wurzburg, O. B. U. S. Patent 2,661,349, 1953.
(29) Bao, J. S.; Xing, J.; Phillips, D. L.; Corke, H. *J. Agric. Food Chem.* **2003**, *51*, 2283−2287.
(30) Kuentz, M.; Egloff, P.; Rothlisberger, D. *Eur. J. Pharm. Biopharm.* **2006**, *63*, 37−43.
(31) Chanamai, R.; and McClements, D. J. *J. Food Sci.* **2001**, *66*, 457−463.
(32) Nilsson, L.; Bergenståhl, B. *J. Agric. Food Chem.* **2007**, *55*, 1469−1474.
(33) Nilsson, L.; Bergenståhl, B. *Langmuir* **2006**, *22*, 8770−8776.
(34) Viswanathan, A. *J. Environ. Polym. Degrad.* **1999**, *7*, 191−196.
(35) Jansson, A.; Järnström, L. *Cellulose* **2005**, *12*, 423−433.
(36) Evangelista, R. L.; Nikolov, Z. L.; Wei, S.; Jane, J. L.; Gelina, R. J. *Ind. Eng. Chem. Res.* **1991**, *30*, 1841−1846.
(37) Bhosale, R.; Singhal, R. *Carbohydr. Polym.* **2006**, *66*, 521−527.
(38) Edwards, D. A.; Brenner, H.; Wasan, D. T. *Interfacial Transport Processes and Rheology*; Butterworth-Heinemann: Boston, MA, 1991.
(39) Erni, P.; Fischer, P.; Windhab, E. J.; Kusnezov, V.; Stettin, H.; Läuger, J. *Rev. Sci. Instrum.* **2003**, *74*, 4916−4924.
(40) Cicuta, P.; Stancik, E. J.; Fuller, G. G. *Phys. Rev. Lett* **2003**, *90*, 236101.
(41) Oh, S. G.; Slattery, J. C. *J. Colloid Interface Sci.* **1978**, *67*, 516−525.
(42) Scriven, L. E. *Chem. Eng. Sci.***1960**, *12*, 98−108.
(43) Boussinesq, M. *Ann. Chim. Phys.* **1913**, *29*, 349.
(44) Larson, R. G. *The Structure and Rheology of Complex Fluids*; Oxford University Press: New York, 1999.
(45) Gunde, R.; Kumar, A.; Lehnert-Batar, S.; Maeder, R.; Windhab, E. J. *J. Colloid Interface Sci.* **2001**, *244*, 113−122.
(46) Martin, A. H.; Cohen Stuart, M. A.; Bos, M. A.; van Vliet, T. *Langmuir* **2005**, *21*, 4083−4089.
(47) Sollich, P.; Lequeux, F.; Hébraud, P.; Cates, M. E. *Phys. Rev. Lett.* **1997**, *78*, 2020.
(48) Bantchev, G. B.; Schwartz, D. K. *Langmuir* **2003**, *19*, 2673−2682.
(49) Trappe, V.; Weitz, D. A. *Phys. Rev. Lett.* **2000**, *85*, 449−452.
(50) Mezzenga, R.; Schurtenberger, P.; Burbidge, A.; Michel, M. *Nat. Mater.* **2005**, *4*, 729−740.
(51) Brooks, C. F.; Fuller, G. G.; Frank, C. W.; Robertson, C. R. *Langmuir* **1999**, *15*, 2450−2459.
(52) Chang, C.; Boger, D. V.; Nguyen, Q. D. *Ind. Eng. Chem. Res.* **1998**, *37*, 1551−1559.
(53) Ng, T. S. K.; McKinley, G. H.; Padmanabhan, M. *Appl. Rheol.* **2006**, *16*, 265−274.

BM700578Z